Reactive Transport Modeling and Characterization of Concrete Materials with Fly Ash Replacement under Carbonation Attack- 15477

J. L. Branch[1], K.G. Brown[1], J. R. Arnold[1], H.A. van der Sloot[2], D.S. Kosson[1]
[1]Vanderbilt University, Dept. of Civil and Environmental Engineering, Nashville, TN
[2]Hans van der Sloot Consultancy, Langedijk, The Netherlands

ABSTRACT

There currently lacks sufficient knowledge to accurately characterize structural, hydraulic, and chemical performance of cementitious materials that are required to contain and shield nuclear waste for thousands of years. There are a number of degradation methods that can affect the integrity of these materials over this time frame including carbonation which lowers the alkalinity of the material and can induce cracking in materials with steel reinforcement. The rate and extent of carbonation in these materials is impacted by the addition of fly ash and its composition which can vary depending on the fly ash source. To characterize the carbonation reaction, the changes in the microstructure and elemental distribution as a function of extent of carbonation and fly ash type were evaluated using scanning electron microscopy (SEM) coupled with energy dispersive x-ray spectroscopy (EDS). Microconcretes were prepared with no fly ash (control case) and with fly ash of various calcium compositions. The progression of the carbonation front was observed in the backscattered electron images by the formation of calcium carbonate and depth was confirmed with a phenolphthalein pH indicator test. The migration and deposition of chemical species were observed in carbonated regions from EDS data and were explained based on the changes in material alkalinity and solubility determined from EPA Method 1313 (Liquid-solid partitioning (LSP) as a function of eluate pH). The changes in mass transport properties from carbonation were observed using EPA Method 1315 (Mass transfer rates in monolithic and compacted granular materials using semi-dynamic tank leaching procedures). The carbonation reaction in each material was simulated using LeachXS/ORCHESTRA, a reactive transport modeling tool, which provided further evidence of localized deposition and migration of chemical species due to changes in speciation and solubility.

INTRODUCTION

Aging Processes

Concrete and other cementitious materials are currently used to immobilize and shield low-level and high-level radioactive waste in applications such as concrete vaults and cementitious waste forms [1-3]. These structures are required to maintain chemical, physical, and hydraulic performance over extended time periods to prevent the unwanted release of radioactive contaminants into the environment. There a number of degradation scenarios that could affect the integrity of these materials, yet there currently lacks a robust knowledge set to accurately model and predict material performance over the long time periods needed for radioactive waste management purposes.

One key degradation scenario that has been identified that could affect the performance of cementitious materials is carbonation [4]. The porous nature of concrete allows for CO_2 diffusion when exposed to either atmospheric air or soil gas. The major reaction that occurs is the formation of calcium carbonate (calcite) from the reaction of calcium hydroxide from the Portland cement with diffused CO_2 (Eq. 1).

$$Ca(OH)_2 + CO_2 \rightarrow CaCO_3 + H_2O \qquad \text{(Eq. 1)}$$

One potential advantage of this reaction is that it can change the pore structure of the material by decreasing the porosity of the concrete leading to an increase in compressive strength. However, carbonation also lowers the alkalinity of the pore solution which, at a pH 9, can depassivate the steel reinforcement inducing corrosion and eventual cracking. Not only does cracking weaken the structural performance of the material, but it also facilitates the transport of infiltrating water and reactive gases into the materials structure, thus accelerating the aging process. Carbonation can also increase the leaching of certain pH-sensitive species (i.e., those that are more soluble at lower pH conditions). Therefore, cracking may also increase the release of these species.

Supplemental Materials

In recent years, there has been an increased emphasis on the use of supplemental cementitious materials (SCMs) in concrete which adds further complexity in predicting the evolution of the carbonation front. Fly ash, one type of commonly used supplemental material, serves as a Portland cement replacement and has been shown to increase material mechanical performance. Environmental benefits of the use of fly ash include a reduction in virgin material mining, a decrease in the carbon footprint associated with Portland cement production, and a decrease in landfill volumes required for fly ash storage. It has been demonstrated that cement replacement by fly ash increases the rate of carbonation in concrete materials [5, 6], but the mechanisms and progression of the carbonation front for the microstructural properties has not been well characterized.

To assess the impact of fly ash as a Portland cement replacement on the geochemical speciation and microstructural properties, microconcrete materials with no fly ash and microconcretes with cement replacement of a low calcium fly ash (FA02), moderate calcium fly ash (FA18), and a high calcium fly ash (FA39) were prepared and exposed to carbonation degradation conditions. The microstructural changes and chemical speciation were observed using scanning electron microscopy coupled with energy dispersive x-ray spectroscopy (SEM-EDS). Localized deposition and migration of chemical species in the carbonated region were linked to changes in chemical speciation and solubility characterized with EPA Method 1313 and 1315 [7] with further evidence supported by simulations from LeachXS/ORCHESTRA, a reactive transport modeling tool [8, 9].

METHODS AND MATERIALS

Components

Three fly ash samples currently used in commercial concrete applications were obtained from a commercial concrete vendor: FA02 (low calcium, bituminous coal ash), FA18 (moderate calcium, sub-bituminous), and FA39 (high calcium, sub-bituminous). SW-846 Method 3052 and Method 3051A were performed by ARCADIAS-US, Inc. (Durham, NC) to determine total sample decomposition. ASTM Type I/II Portland cement and river sand (fine aggregate) were obtained from a commercial concrete vendor and used in all concrete formulations [10].

Microconcrete formulation and preparation

A control microconcrete containing no fly ash (M-45-00) and a microconcretes with a 45% fly ash replacement levels of the Portland cement of each fly ash sample (M-45-02, M-45-18, M-45-39) were prepared (Table I). The water-to-binder ratio was fixed at 0.45 for both material types. Microconcretes have previously served as surrogates for concrete materials containing coarse aggregate because they are easier to handle for testing such as the LEAF methods because they lack coarse aggregate. Concrete components are adjusted in amounts necessary to maintain the aggregate-paste interfacial area expected for concrete materials with coarse aggregate.

Three sets of microconcrete samples were cured by placing each monolith on a stand above a 1 inch water level and sealed for 6 months. One set of the M-45-00, M-45-02, M-45-18, and M-45-39 were cured for an additional 6 months, one set of the M-45-00, M-45-02, M-45-18, and M-45-39 were carbonated in a 5% CO_2 chamber at 65% relative humidity for 6 months (MC-45-00, MC-45-02, MC-45-18, and MC-45-39, respectively), and one set was crushed after curing and then carbonated for 6 months at the same conditions (granular MC-45-00, MC-45-02, MC-45-18, and MC-45-39). The granular carbonated samples served as the carbonated material in EPA Method 1313 so that all exposed surface areas in the test were carbonated.

TABLE I. Microconcrete formulations

	Control	**Blend**
Nominal Mix (lb/cy)	866	866
Fly ash replacement	-	45
Composition (wt%)		
Portland Cement	22.2	12.2
Fly ash	-	10
Water	9.9	10.1
Fine Aggregate	67.9	67.7
Material Code	MC-45-00	MC-45-02, MC-45-18, MC-45-39

SEM Sample Preparation

A 5 millimeter wide and 10 millimeter long section from the interior of the exposed surface measuring 5 millimeters in depth from the exposed surface was removed from each monolith. The samples were exchanged with ethanol to remove any remaining pore water and to stop the hydration reaction.

All samples were prepared using 1 ¼ inch diameter Allied SEM molds (Allied High Tech Products, Inc. Rancho Dominguez, CA) with material embedded in a 4:1 EpoHeat epoxy resin to EpoHeat epoxy hardener (Buehler, Lake Bluff, IL) ratio to provide a structural support and allow for sample polishing. Samples were oriented in the mold so that a cross-section in the direction from the exposed surface would be observed. The molds were covered with wax and placed in a 55 degrees Celsius incubator for 48 hours to allow for complete hardening.

Samples were removed from the molds and flattened until level using A-99 240 grit sand paper. A series of polishing steps with increasingly finer grade sand paper and polishing cloths was implemented to obtain a smooth, flat sample surface using the Allied METPREP 3-PH Grinding/Polishing system with the BlueLube polishing lubricant (Allied High Tech Products, Inc. Rancho Dominguez, CA). Polishing cloths were intermittently sprayed with the lubricant to maintain a moist polishing pad. Samples were lightly rinsed with ethanol in between each cloth exchange. Samples were ultrasonically cleaned in ethanol for 60 seconds after the final polishing step and mounted on an aluminum stub with a carbon tape adhesive.

SEM-EDS Analysis

All samples were collected at 10 keV with a spot size of 3.5 and a working distance of 10.0 mm using a Phillips/FEI Quanta 650 field emission electron microscope in ESEM mode with a 130 Pa chamber pressure to prevent charging. A 10 keV energy exceeds the excitation energy levels for the major elements in concrete and fly ash materials that is required to produce the characteristic x-ray peaks for qualitative analysis. Inca software from the Oxford Software Suite was used to collect and process EDS data. A beam optimization was performed on a titanium standard for 60 seconds. Backscattered images of 1024 x 943 pixel resolution and EDS maps of 256 x 224 resolution were collected at each samples site. A horizontal field width (HFW) of 256 microns was chosen out of convenience to convert pixel measurements into microns. This HFW corresponds to a Polaroid magnification of 496 and is appropriate to capture finer details of the fly ash particles, calcium carbonate precipitate, unhydrated Portland cement particles, and other microstructural features of carbonated cement paste, yet large enough to observe portions of fine aggregate features. 1000 EDS frames per site were collected with a dwell time of 100 µs per pixel. EDS maps were quantified using a set of reference standards and the titanium beam optimization.

During SEM-EDS mapping, samples were oriented so that the exposed surface was parallel with the field of view. Multiple maps were collected moving perpendicular from the exposed surface until the non-carbonated region was observed. Backscattered images and EDS data were coupled together to measure and observe the carbonation profile. Heat maps of the ratio of calcium to aluminum plus silica were used to normalize EDS data. Normalization is used to

account for changes in material density and presence of hydrated phases that can influence the measurable counts in the EDS spectrum.
A phenolphthalein test was used to estimate the carbonation depths of each sample and compare to results from SEM-EDS. A stock solution of 0.1 g phenolphthalein per 100 ml of ethanol was prepared and used on each sample. The carbonation depth was estimated by measuring the distance of the sample that did not change color which indicates a drop in pH below 10.

LeachXS/ORCHESTRA Modeling

LeachXS/ORCHESTRA includes a geochemical/reactive transport model that was used to simulate the diffusion of CO_2 and the resulting pore space reactions and constituent leaching [8, 9] for a control (MC-45-00) and microconcrete (MC-45-02) with low calcium fly ash replacement (Table I). A two-layer, one-dimensional version of the model with no-flux boundaries (Figure 1) was used to evaluate the basic diffusional transport of species within the microconcretes. One layer represented a pre-carbonated representation of the microconcrete under study. Other important transport phenomena (e.g., gaseous diffusion, pore structure changes, rebar corrosion, and water and associated ionic transport due to different capillary pressures across the concrete-soil interface) will be considered in future studies. EPA Methods 1313 (equilibrium pH test) and 1315 (mass transfer test) were performed on all non-carbonated (M-45-00, M-45-02, M-45-18, and M-45-39) and carbonated materials (granular MC-45-00, MC-45-02, MC-45-18, and MC-45-39). The mean availabilities from two repetitions (A and B) in EPA Method 1313 were used in the modeling.

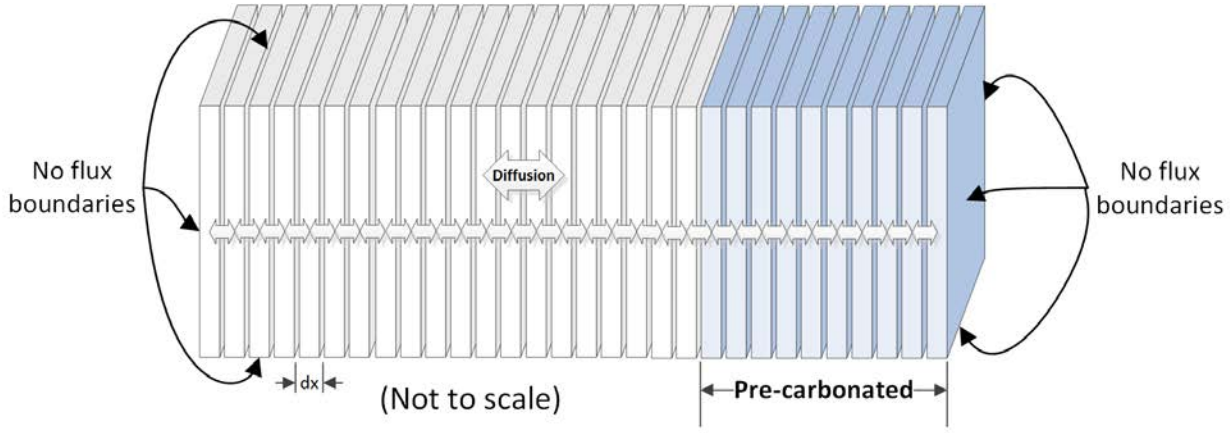

Fig. 1: LeachXS/ORCHESTRA model used in this study. Note the area to the right has been pre-carbonated and all edges represent no-flux boundaries.

RESULTS

EPA Methods 1313 and 1315
A decrease in the solubility of calcium was observed for carbonated materials compared to the noncarbonated materials at each material's natural pH using EPA Method 1313 (Table II). A decrease in the calcium solubility was also observed at other pH values between 6 and 13.5 for carbonated materials (Figure 1.A-B; data not shown for M-45-18, MC-45-18, M-45-39, and MC-45-39).

TABLE II. Mean pH and Ca Solubility from EPA Method 1313 for Non-Carbonated (M-45-##) and Carbonated Materials (MC-45-##)

Material	Mean Natural pH	Mean Ca Solubility (mg/L)
M-45-00	12.66	902
MC-45-00	12.12	156
M-45-02	12.79	724
MC-45-02	10.28	117

EPA Method 1315 revealed a significant decrease in the mass transfer rate of calcium for carbonated materials compared to non-carbonated materials (Figure 2.C-D). As time increased, the difference between mass transfer rates of carbonated and non-carbonated materials decreased for both material types.

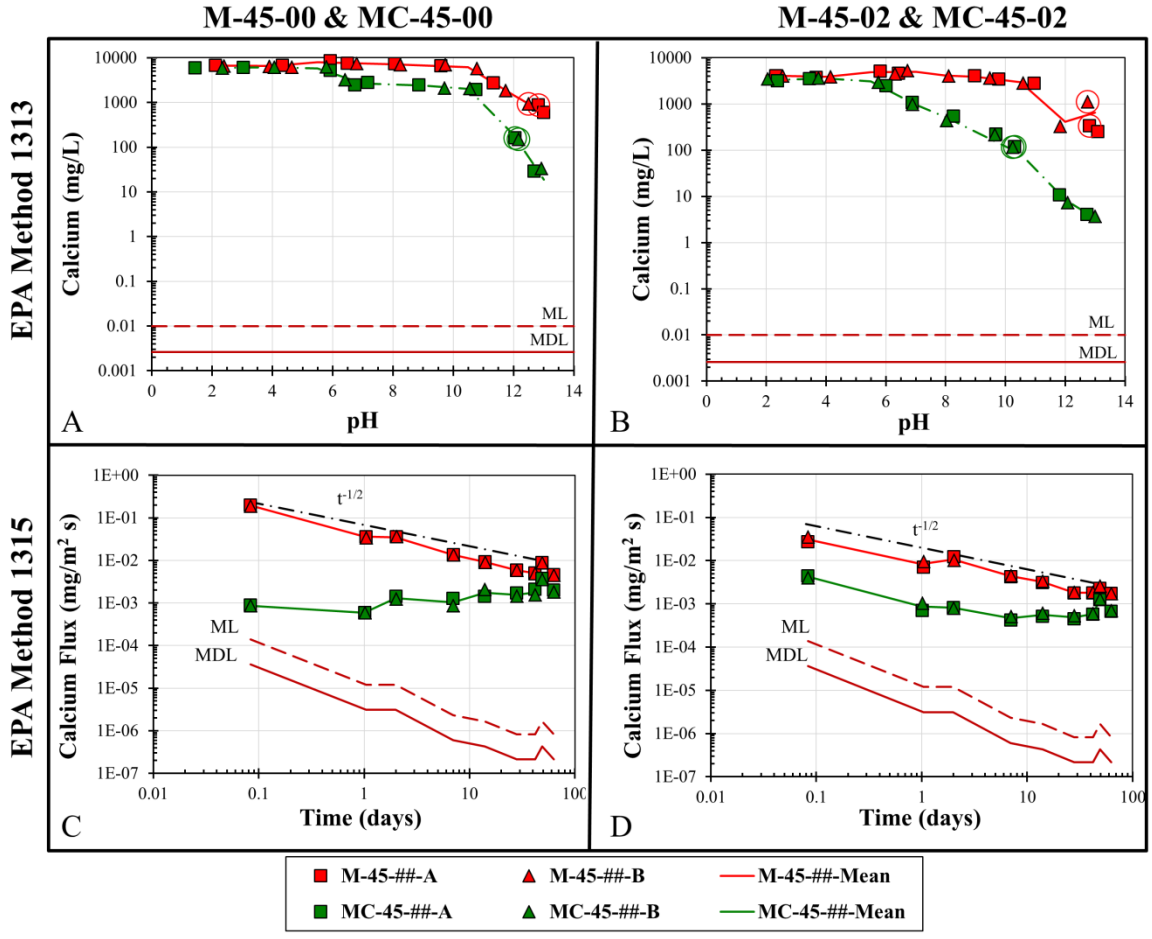

Fig. 2.A-D: pH equilibrium test results from EPA Methods 1313 for (A) M-45-00 & MC-45-00 and (B) M-45-02 & MC-45-02 and mass transfer results from EPA Method 1315 for (C) M-45-00 & MC-45-00 and (D) M-45-02 & MC-45-02

Carbonation Profile from Phenolphthalein Test

Phenolphthalein test revealed observable carbonation depths on the millimeter scale (Figure 3.A&B). The mean carbonation depth was 0.4 mm for MC-45-00 and 1.2 mm for MC-45-02. The carbonated layer was observed to be non-uniform across the surface do to the presence of fine aggregates at the exposed surface.

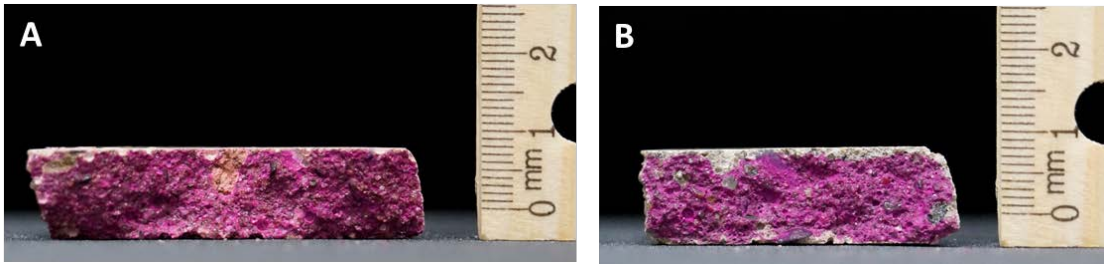

Fig. 3.A&B: Carbonation front of microconcrete monolith samples observed from phenolphthalein pH indicator test A) MC-45-00 B) MC-45-02 orientated so that the exposed surface is at the top of the microconcretes. Bright pink regions indicate a pH range above 10 and clear regions indicate a drop in pH below 10.

SEM-EDS Carbonation Profile

Backscattered images revealed formation of calcium carbonate near the exposed surface area for both microconcretes. Calcium carbonate appeared as large lighter gray regions dispersed throughout the darker unreacted calcium hydroxide cement paste. The non-carbonated region appeared darker and did not show the presence of calcium carbonate. The transition zone between the carbonated and non-carbonated regions is shown in Figure 4 to highlight the microstructural differences. The elemental weight distribution determine by EDS data for the calcium carbonated observed in the backscattered image agreed with the elemental weight distribution expected for calcium carbonate.

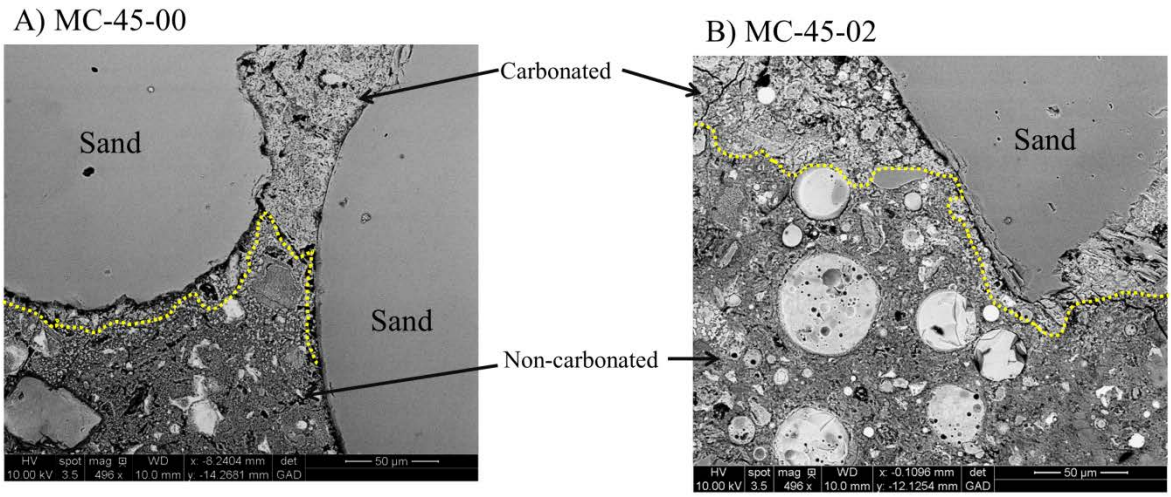

Fig. 4. A&B: Transition zone between the carbonated region (above yellow dotted line) and the non-carbonated region (below yellow dotted line) for (A) MC-45-00 and (B) MC-45-02.

EDS heat maps revealed an increase in the ratio of calcium to aluminum + silica in the carbonated regions (Figure 5. B&D) as identified by the presence of calcium carbonate in the backscattered image (Figure 5.A&C). MC-45-00 exhibited higher ratios of calcium to aluminum + silica in both carbonated and non-carbonated regions compared to MC-45-02 due to the initial greater concentration of calcium in the material. The carbonation depth was 0.5 millimeters for MC-45-00 and 1.7 millimeters for MC-45-02 which corresponds similarly to the depths observed by the phenolphthalein test (Table III).

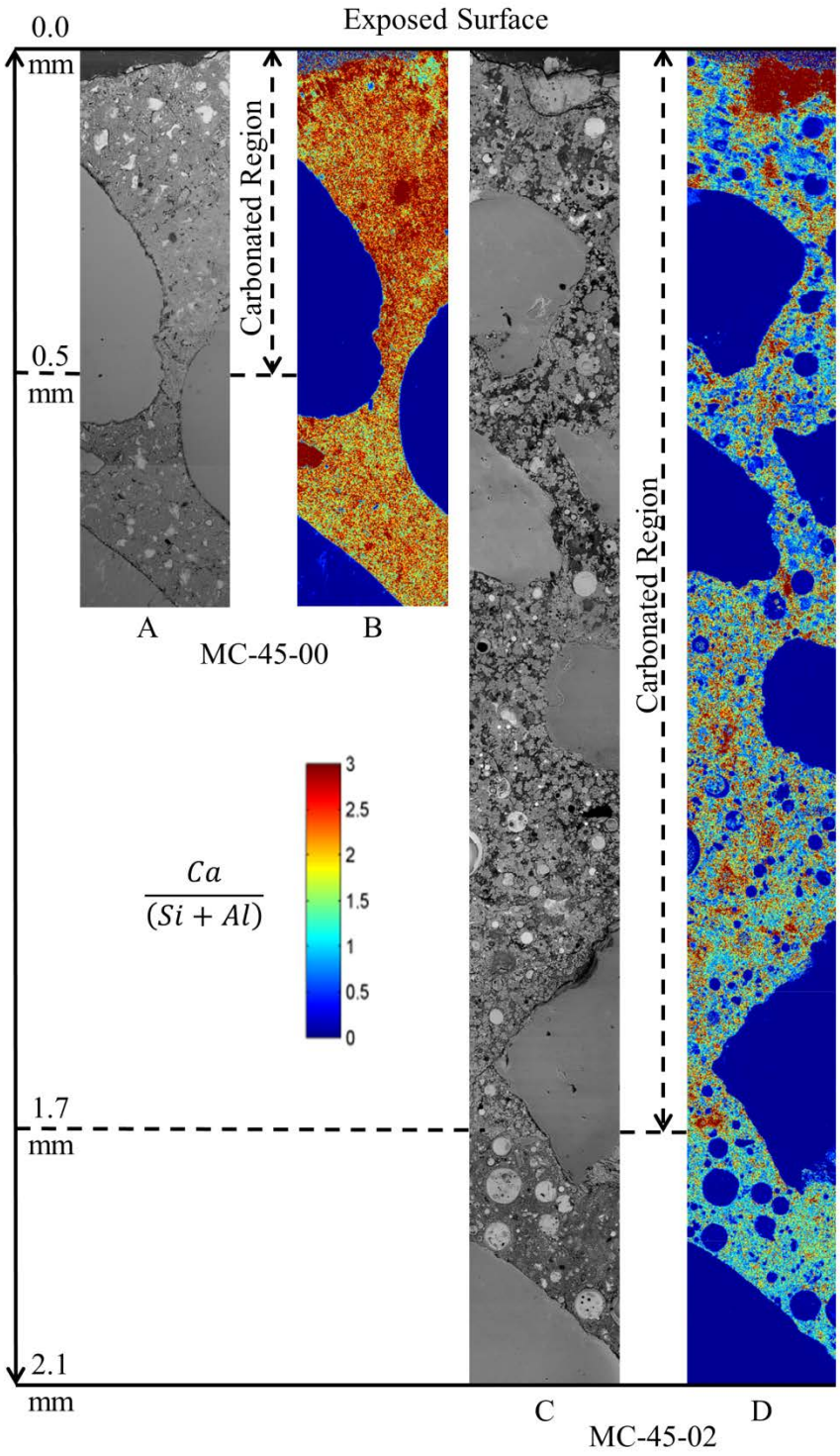

Fig. 5.A-D: Carbonation profiles observed in the backscattered images A) MC-45-00 C) MC-45-02 and in the EDS heat maps for Ca/(Al+Si) B) MC-45-00 D) MC-45-02. The exposed surface to CO_2 conditions is at 0.0 mm with increased distances representing an increase in distance from the exposed surface.

TABLE III: Mean carbonation depths (millimeters) for MC-45-00 and MC-45-02

	Phenolphthalein	SEM-EDS
MC-45-00	0.4	0.5
MC-45-02	1.2	1.7

LeachXS/ORCHESTRA

The predicted pH and pore solution Ca^{+2} results from the LeachXS/ORCHESTRA simulations for the MC-45-00 (control) and MC-45-02 (low calcium fly ash replacement) are provided in Figure 6 and Figure 7, respectively. In Figure 6, a migration of OH^- ions into the pre-carbonated area (i.e., from left to right) causes the pH to increase over time where the pH effect is more pronounced in the microconcrete (MC-45-02) with fly ash replacement. A corresponding movement of Ca^{+2} ions is observed in Figure 6 from the area of higher solubility (non-carbonated region) to the area of lower solubility (pre-carbonated region). The resulting effect is a deficit of Ca^{+2} at the non-carbonated side of the interface and reprecipitation at the front where the deficit is lower for the microconcrete (MC-45-02) with fly ash replacement. A similar effect is observed with those constituents (e.g., Sr) where solubility and partitioning is a function of pH and degree of carbonation.

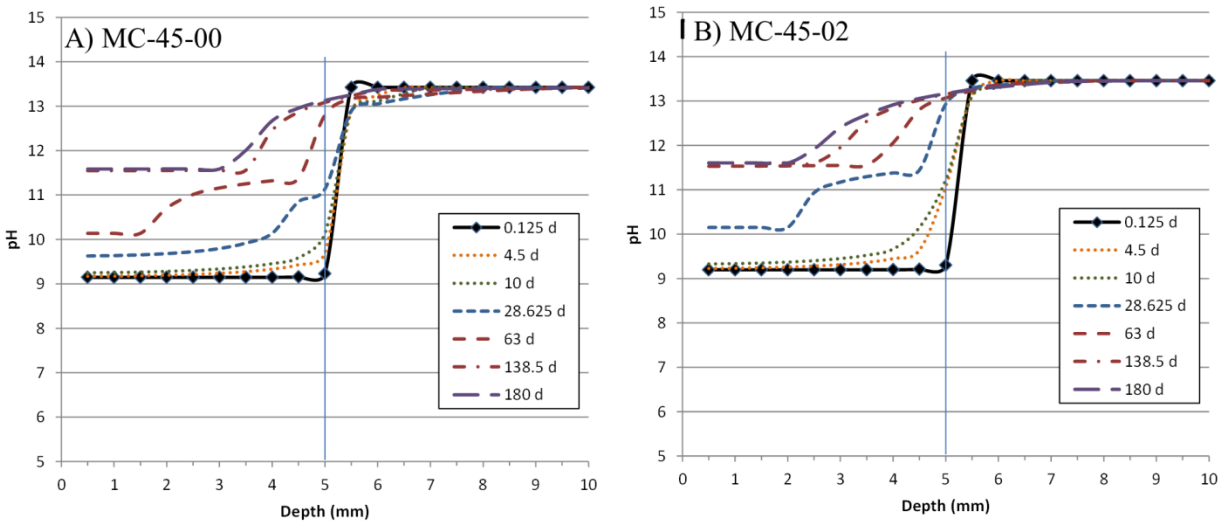

Fig. 6: Predicted pH results for A) MC-45-00 and B) MC-45-02 for a saturated, no flux boundary condition using LeachXS/ORCHESTRA. Note the area 0-5 mm is pre-carbonated.

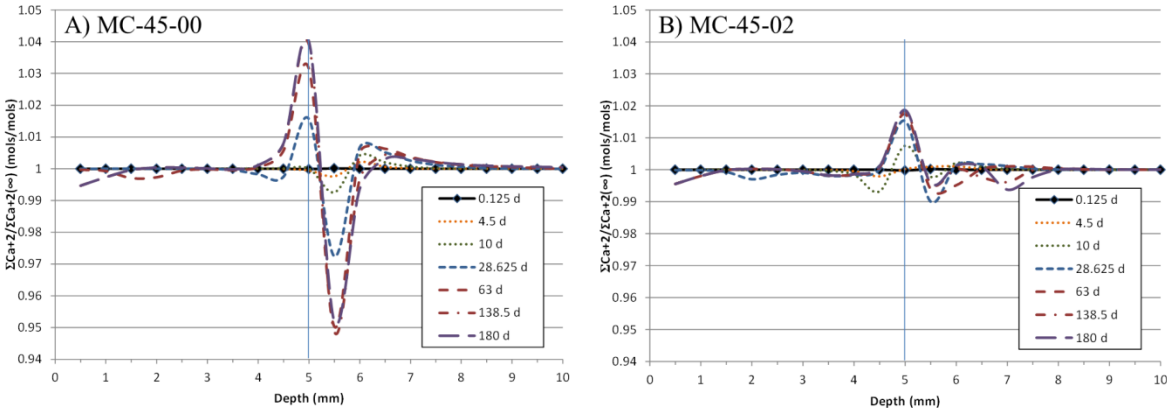

Fig. 7: Predicted normalized calcium results for A) MC-45-00 and B) MC-45-02 for a saturated, no flux boundary condition using LeachXS/ORCHESTRA. Note the area 0-5 mm is pre-carbonated. Note the concentrations are relative to that (denoted Ca+2(∞)) in the material where there is no observed effect of carbonation.

DISCUSSION

Microstructural Changes

The microstructure of calcium carbonate appeared as light gray regions that were dispersed throughout the unreacted hydrated cement paste. Both carbonated microconcretes exhibited similar formation of this phase on the microstructural level which indicates similar carbonation precipitate across both material types.

The heterogeneity of these materials leads to a non-uniform carbonation front. The carbonation front appeared to follow fine aggregates in the material as observed in both backscattered images and by the phenolphthalein test. Carbonation reached greater depths at the boundary of these materials because the carbonation front developed around the materials. It is well known that the interfacial region is the weakest portion of the microconcrete material and exhibits a higher porosity than the mean porosity of the material [11]. Therefore, CO_2 gas can diffuse more rapidly through these regions, thus facilitating the carbonation reaction at deeper regions than typical of the cement paste. In addition, fine aggregates are mostly a silica oxide and therefore have no availability to participate in the carbonation reaction. The CO_2 gas in these interfacial regions can only react with the calcium hydroxide at this boundary, thus creating a preferential reaction direction.

The increase of calcium in the carbonated regions observed in the EDS heat maps and a decrease in the solubility and mass transfer rates of calcium for carbonated materials measured by EPA Method 1313 and EPA Method 1315 suggests a migration of calcium from the more soluble non-carbonated regions to the less soluble carbonated regions. This can be explained by the dissolution of the more soluble calcium hydroxide phase during reaction with the CO_2 to form a less soluble calcium carbonate phase. The mass transfer rates of the carbonated materials

approaching that of the non-carbonated materials at greater times as measured by EPA Method 1315 suggest that the leaching front surpasses the carbonated regions.

Impact of Material Alkalinity

The formation of calcium carbonate was observed at greater depths for the material with fly ash which indicates that a change in the material alkalinity influences the reaction rate of CO_2 gas with the calcium hydroxide. Lower material alkalinity decreases the availability of calcium hydroxide per material volume, therefore the reaction proceeds more rapidly through the material with fly ash.

LeachXS/ORCHESTRA

Modeling results from LeachXS/ORCHESTRA support the experimental findings of calcium migration from the non-carbonated region (higher solubility) to the carbonated region (lower solubility) and reprecipitation due to a change of pH from the carbonation reactions.

CONCLUSION

SEM-EDS experimental results show that a decrease in material alkalinity due to fly ash replacement of the Portland cement increases the depth of carbonation. This carbonation front forms non-uniformly across the material due to the heterogeneity of the microstructure from the presence of fine aggregates. Migration of calcium from the non-carbonated region to the carbonated region observed by SEM-EDS results for the microconcretes was supported by LeachXS/ORCHESTRA modeling results.

ACKNOWLEDGEMENTS

This document is partially based on work supported by the U. S. Department of Energy, under Cooperative Agreement Number DE-FC01-06EW07053 entitled ‘The Consortium for Risk Evaluation with Stakeholder Participation III awarded to Vanderbilt University, David S. Kosson, principal investigator and Charles W. Powers, co-principal investigator. The opinions, findings, conclusions, or recommendations expressed herein are those of the authors and do not necessarily represent the views of the Department of Energy or Vanderbilt University. Disclaimer: This document was prepared as an account of work sponsored by an Agency of the United States Government. Neither the United States Government nor any agency thereof, nor any of their employees, makes any warranty, express or implied, or assumes any legal liability or responsibility for the accuracy, completeness, or usefulness of any information, apparatus, product, or process disclosed, or represents that its use would not infringe privately owned rights. Reference herein to any specific commercial product, process, or service by trade name, trademark, manufacturer, or otherwise does not necessarily constitute or imply its endorsement, recommendation, or favoring by the United States Government or any agency thereof.

REFERENCES

1. Walton, J.C., L.E. Plansky, and R.W. Smith, *Models for Estimation of Service Life of Concrete Barriers in Low-Level Radioactive Waste Disposal*. September 1990, Idaho National Engineering Laboratory, U.S. Department of Energy: Idaho Falls, ID.
2. Seitz, R.R., et al., *Summary of Department of Energy and Nuclear Regulatory Commission Performance Assessment Approaches*, Volume 1: Modeling of Cementitious Barriers, CBP-TR-2009-001, Rev. 0, in Overview of the U.S. Department of Energy and Nuclear Regulatory Commission Performance Assessment Approaches, Cementitious Barriers Partnership, Aiken, SC and Nashville, TN. Available from: http://cementbarriers.org/. 2009.
3. Brown, K.G., et al., *Summary of Department of Energy and Nuclear Regulatory Commission Performance Assessment Approaches*, Volume 2: Sensitivity and Uncertainty Analysis, CBP-TR-2009-001, Rev. 0, in Overview of the U.S. Department of Energy and Nuclear Regulatory Commission Performance Assessment Approaches, Cementitious Barriers Partnership, Aiken, SC and Nashville, TN. Available from: http://cementbarriers.org/. 2009.
4. Snyder, K.A.e., *Engineered Infills for Concrete Barriers*. 2006, National Institute of Standards and Technology: Gaithersburg, MD.
5. Papadakis, V.G., *Effect of supplementary cementing materials on concrete resistance against carbonation and chloride ingress.* Cement and Concrete Research, 2000. **30**(2): p. 291-299.
6. Khunthongkeaw, J., S. Tangtermsirikul, and T. Leelawat, *A study on carbonation depth prediction for fly ash concrete.* Construction and Building Materials, 2006. **20**(9): p. 744-753.
7. Garrabrants, A.C., et al., *Background information for the Leaching Enviornmental Assessment Framework (LEAF) Test Methods.* EPA-600/R-10/170, U.S. Environmental Protection Agency, Air Pollution Prevention and Control Division, December 2010.
8. Meeussen, J.C.L., *ORCHESTRA: An Object-Oriented Framework for Implementing Chemical Equilibrium Models.* Environmental Science & Technology, 2003. **37**(6): p. 1175-1182.
9. Kosson, D.S., et al., *Application of the New US EPA Leaching Environmental Assessment Framework (LEAF) to DOE Environmental Management Challenges*, in *Waste Management Symposia 2014*. Phoenix, AZ.
10. Kosson, D.S., et al., *pH-dependent leaching of constituents of potential concern from concrete materials containing coal combustion fly ash.* Chemosphere, 2014. **103**(0): p. 140-147.
11. Scrivener, K., A. Crumbie, and P. Laugesen, *The Interfacial Transition Zone (ITZ) Between Cement Paste and Aggregate in Concrete.* Interface Science, 2004. **12**(4): p. 411-421.